



Available online at

Journal of Science and Technology

E-ISSN



Gamow-teller strength and electron capture cross-section calculation by pn-QRPA for selected fp-shell nuclei

Jameel-Un Nabi^a, * , Muhammad Riaz^a , Asim Ullah^a 

^a GIK Institute of Engineering Sciences and Technology, Topi 23640, Khyber Pakhtunkhwa, Pakistan.

ARTICLE INFO

Article history:

Received 30 October 2019

Received in revised form 09 December 2019

Accepted 05 April 2020

Keywords:

Gamow-Teller transitions
electron capture cross section
pn-QRPA theory;
stellar evolution

ABSTRACT

The allowed Gamow-Teller (GT) strengths and associated weak interaction rates on fp-shell nuclides are the most familiar processes of spin-isospin ($\sigma\tau$) type. These rates play crucial role in several astrophysical processes, particularly in nuclear synthesis and supernova-explosions. As per simulation consequences, the electron capture cross section on medium-heavy nuclei has a key impact on decreasing the ratio of electron-to-baryon of the stellar matter during the late stages of stars formation. Stellar model based on the theoretical approaches should be tested against the available measured data. In the current work we present calculated Gamow-Teller strength distributions by pn-QRPA model for selected fp-shell nuclei (^{42}Ti , ^{46}Cr , ^{50}Fe and ^{54}Ni) and compare our results with available measured data. The Gamow-Teller strength distributions are well fragmented over the energy range 0-12 MeV and have a good comparison with experimental data. We calculate the electron capture cross-section for selected nuclei at temperature 0.5 MeV, 1.0 MeV and 1.5 MeV that shows the temperature dependence of calculated electron capture cross section for astrophysical applications.

© 2020. Turkish Journal Park Academic. All rights reserved.

1. Introduction

In study of nucleosynthesis and other astrophysical processes, beta decay plays an important role in analysis of Gamow-Teller (GT) transitions and nuclear half-lives. The GT transitions may be investigated by charge-changing transition reactions under laboratory conditions. But data for GT transitions for most of the unstable nuclei may be provided by many of the theoretical models possessing a decent agreement with experimental data. One such successful nuclear model is the proton-neutron quasi-particle random phase approximation (pn-QRPA) model that provides weak interactions rates under terrestrial as well as stellar conditions [1-4].

Fuller, Fowler, and Newman [5], computed the beta decay weak interactions rates for the first time by using independent particle model (IPM). They tabulated the beta decay rates for many nuclei ($21 \leq A \leq 60$) having importance in astrophysical

applications. Later large scale shell model diagonalization model, Shell Model Monte Carlo [6, 7] and pn-QRPA models refined the weak interaction rates for simulation of pre-supernova phenomenon [3, 8, 9]. By improving these weak interaction rates it was concluded that GT strength distributions and electron capture cross-sections (ECC) for fp-shell nuclei play crucial role in providing information for pre-supernova evolution of massive stars.

In this article, we compute GT transitions and ECC for selected fp-shell nuclei by pn-QRPA model. In performing our calculation, we used state by state computation instead of Brink's-Axel hypothesis [10].

* Corresponding author.

E-mail address: jameel@giki.edu.pk

ORCID: 0000-0002-8229-8757 (Jameel-un Nabi), 0000-0003-4521-4259 (Muhammed Riaz), 0000-0002-2653-310X (Asim Ullah)

2. Formalism

The pn-QRPA model was used to compute the GT strength distribution and associated ECC on the selected chromium isotopes in the stellar matter. The following Hamiltonian was considered

$$H^{\text{QRPA}} = H^{\text{sp}} + V_{\text{GT}}^{\text{ph}} + V_{\text{GT}}^{\text{pp}} + V^{\text{pair}}, \quad (1)$$

where H^{sp} is the single particle Hamiltonian, $V_{\text{GT}}^{\text{ph}}$ and $V_{\text{GT}}^{\text{pp}}$ are the particle-hole GT force and particle-particle GT force, respectively. The last term V^{pair} represents the pairing force for which the BSC approximation was considered. The single particle energies and wave functions were calculated in Nilsson model [11], in which the nuclear deformation (β_2) was incorporated. The particle-particle and particle-hole parameters were adapted such that the measured energy of the GT giant resonance was reproduced wherever available. The calculated GT strength distributions fulfilled the model independent Ikeda sum rule [12]. The Nilsson-potential parameter (NPP) was taken from Ref. [13] and $\hbar\omega = 41A^{1/3}$ was taken as oscillator constant for both neutrons and protons. Q-values were taken from Ref. [14] and a traditional relation $\Delta_p = \Delta_n = 12/\sqrt{A}$ MeV was considered for pairing gaps. The electron capture (EC) and positron decay (PD) weak-rates from parent state “m” to daughter state “n” are given by

$$\lambda_{\text{mn}}^{\text{EC(PD)}} = \ln 2 \frac{f_{\text{mn}}^{\text{EC(PD)}}(T, \rho, E_f)}{D/B_{\text{mn}}}, \quad (2)$$

where B_{mn} is the nuclear reduced transition probability and is given by

$$B_{\text{mn}} = B(\text{F})_{\text{mn}} + (g_A/g_V)^2 B(\text{GT})_{\text{mn}}. \quad (3)$$

The values of D and g_A/g_V were taken as 6143s [15] and -1.254 [16], respectively. The reduced Fermi ($B(\text{F})_{\text{mn}}$) and GT ($B(\text{GT})_{\text{mn}}$) transition probabilities are specified by the following

$$B(\text{F})_{\text{mn}} = \frac{1}{2J_{m+1}} |\langle n || \sum_k t_+^k || m \rangle|^2, \quad (4)$$

$$B(\text{GT})_{\text{mn}} = \frac{1}{2J_{m+1}} |\langle n || \sum_k t_+^k \sigma^{-k} || m \rangle|^2, \quad (5)$$

where J_m is the total spin of the parent state $|m\rangle$, σ^{-k} is the Pauli spin matrix and t_+^k refer to the iso-spin raising operator. The summation is taken for all the nucleons inside the nucleus. The computation of electron capture cross-section is governed by the weak-interaction Hamiltonian, given by

$$\hat{H}_\omega = \frac{G_F \cos \theta_c}{\sqrt{2}} j_\mu^{\text{lept}} j^\mu, \quad (6)$$

The terms θ_c and G_F in the above equation, stands for Cabibbo angle and Fermi coupling constant, respectively. The j^μ and j_μ^{lept} are the hadronic and leptonic currents, respectively, given by

$$j_\mu^{\text{lept}} = \bar{\Psi}_{\nu_e}(x) \gamma_\mu (1 - \gamma_5) \Psi_{\nu_e}(x), \quad (7)$$

$$j^\mu = \bar{\Psi}_p(x) \gamma_\mu (1 - C_A \gamma_5) \Psi_n(x), \quad (8)$$

where $\Psi_{\nu_e}(x)$ show the spinor operator. Our main goal was to compute the ECC which is based on nuclear transition matrix elements between initial $|m\rangle$ and final state $|n\rangle$ of parent and daughter nuclei, respectively.

$$\langle n || \hat{H}_\omega || m \rangle = \frac{G}{\sqrt{2}} l^\mu \int d^3x e^{-iq \cdot x} \langle n || j_\mu || m \rangle \quad (9)$$

where the q is the three-momentum transfer and $l^\mu e^{-iq \cdot x}$ are the leptonic matrix element which was employed in matrix elements calculation [17, 18]. We used low momentum transfer approximation $q \rightarrow 0$ in this work. By assuming such approximation the transitions of Gamow-Teller (GT) operator ($\text{GT}^+ = \sum_i \tau_i^+ \sigma_i$) provide the dominant contribution to the total stellar ECC [19]. The total ECC in the stellar condition as a function of incident energy of projectile electron (E_e) is given by the equation

$$\sigma(E_e, T) = \frac{G_F^2 \cos^2 \theta_c}{2\pi} \sum_m F(Z, E_e) \frac{(2J_{m+1}) \exp(-\frac{E_m}{kT})}{G(A, Z, T)} \times \sum_{j,f} (E_e - Q + E_m - E_m)^2 \frac{|(m | \text{GT}^+ | n)|^2}{(2J_{m+1})} \quad (10)$$

The terms $F(Z, E_e)$ and $G(A, Z, T)$ are the well-known Fermi and nuclear partition function (NPF), respectively. The last term of Eq. (10) corresponds to the nuclear matrix elements between final and initial states. The calculation of Fermi function was done using the recipe given by Ref. [19]. The NPF was computed using the prescription introduced by Refs. [20, 21].

3. Results and Discussion

The GT strength distributions computed by pn-QRPA for ^{42}Ti , ^{46}Cr , ^{50}Fe and ^{54}Ni are compared with the experimental data and previous calculations [22-28] in Fig. 1. In β -decay experiment the excitation energy up to $E_{\text{ex}} = 1.888$ MeV was considered to probe the GT strength distributions while in charge changing reaction $^{42}\text{Ca}(^3\text{He}, t)$ a maximum of $E_{\text{ex}} = 3.688$

MeV was considered to measure the GT strength.

In Fig. 1 we also depict shell model (using GXPF1 and KB3G interactions) and pn-QRPA extended GT strength distributions up to $E_{ex} = 12$ MeV. Calculated GT strength distribution by pn-QRPA have good fragmentation for all energy range up to 12 MeV and are bigger in magnitude than previously calculated and measured results. One notes a decent comparison of the measured and calculated GT strength distributions.

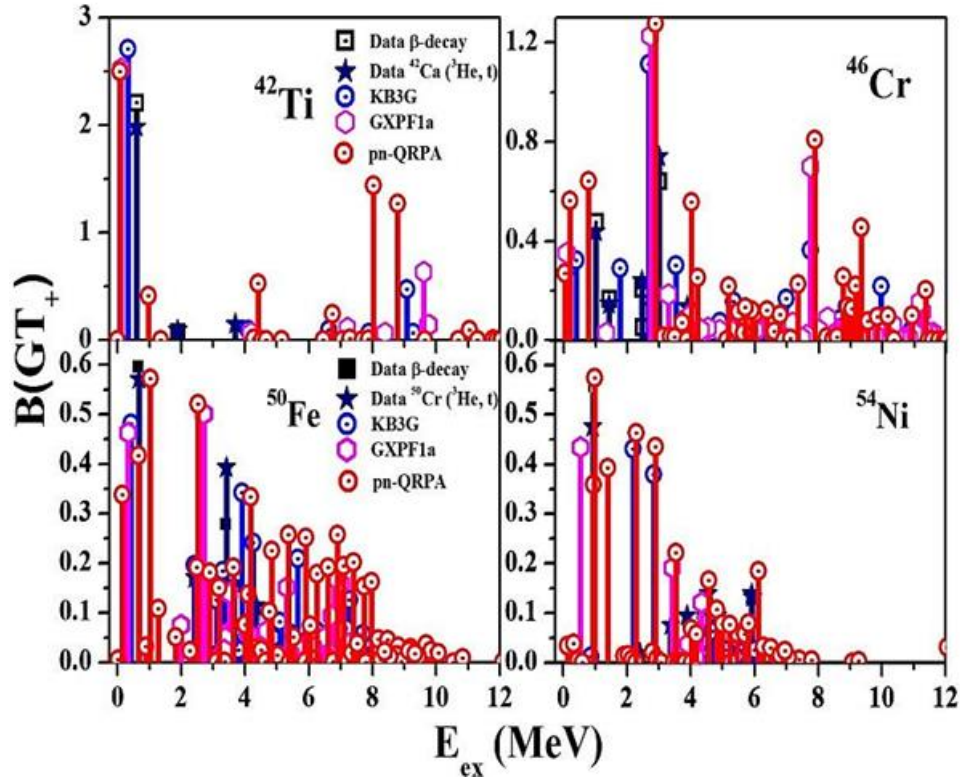


Figure 1. Calculated and measured GT strength distributions for ^{46}Cr , ^{54}Ni , ^{50}Fe and ^{42}Ti as a function of daughter excitation energy. For explanation of legends see text.

Table 1 show the measured and computed GT strength distribution for ^{54}Ni , ^{50}Fe , ^{46}Cr , and ^{42}Ti . The third and fourth column of Table 1 shows the experimental data of β -decay and charge changing reaction, 5th and 6th column represents the shell model data calculated through KB3G and GXPF1

interactions, respectively. Second last and last column display the results of extreme single particle model and pn-QRPA. The difference between measured and calculated data is attributed to the cut-off energies described before. It is noted that the pn-QRPA and extreme single particle model results are bigger than the results of other models.

Table 1. Comparison of measured and computed total GT strengths for selected fp-shell nuclei.

A	N	β -Decay	CER	KB3G	GXPF1a	ESPM	pn-QRPA
54	26	1.082	1.117	12.197	13.362	16.29	18.16
50	24	1.344	1.859	9.464	10.277	14.14	16.97
46	22	2.047	2.219	7.231	7.613	10.70	9.50
42	20	2.372	2.297	6.000	6.000	6.00	7.86

In the last part of our article we describe the results of ECC for selected fp-shell nuclei (^{42}Ti , ^{46}Cr , ^{50}Fe and ^{54}Ni) achieved by employing the pn-QRPA model. These results are shown in Table 2 (^{42}Ti and ^{46}Cr) and Table 3 (^{50}Fe and ^{54}Ni). The calculated ECC is shown as a function of incident electron energy at three different temperature 0.5 MeV, 1.0 MeV and 1.5 MeV. In Table 2 and Table 3 the first column shows the incident electron energy. Further three different temperatures are mentioned for all of nuclei in both the tables.

The comparison of ECC for all selected cases shows almost same trend. As the incident electron energy increases the ECC for the first few MeV increases sharply. This trend in calculated ECC later becomes smooth with further increase in incident electron energy. The calculated ECC have direct impact on GT

strength distributions and therefore this trend may be a direct consequence of the calculated GT strength distributions.

To study the effect of ECC on temperature we calculated ECC at three effective temperatures in the range of 0.5 MeV – 1.5 MeV. As the temperature of the core increases from 0.5 MeV to 1.5 MeV the calculated ECC increased on average by two orders of magnitude. This big change is because of thermal unblocking of GT states. As the temperature further increases from 1.0 MeV to 1.5 MeV the calculated ECC increased marginally as the unblocking of states has already taken place. The trend of the calculated ECC is similar for all four cases.

Table 2. Calculated EC cross section (in units of cm^2) for three different temperatures 0.5MeV, 1.0MeV and 1.5MeV for ^{42}Ti and ^{46}Cr .

Energy (MeV)	^{42}Ti			^{46}Cr		
	T=0.5MeV	T=1.0MeV	T=1.5MeV	T=0.5MeV	T=1.0MeV	T=1.5MeV
2	2.25E-48	3.14E-47	3.97E-47	3.39E-48	4.31E-47	5.75E-47
3	5.01E-47	6.97E-46	8.80E-46	7.70E-47	9.79E-46	1.31E-45
4	3.25E-46	4.48E-45	5.66E-45	5.05E-46	6.42E-45	8.57E-45
5	1.22E-45	1.67E-44	2.11E-44	1.91E-45	2.44E-44	3.26E-44
6	3.33E-45	4.54E-44	5.75E-44	5.27E-45	6.74E-44	9.01E-44
7	7.40E-45	1.00E-43	1.28E-43	1.17E-44	1.51E-43	2.03E-43
8	1.42E-44	1.93E-43	2.46E-43	2.24E-44	2.91E-43	3.93E-43
9	2.46E-44	3.37E-43	4.33E-43	3.81E-44	5.04E-43	6.83E-43
10	3.98E-44	5.54E-43	7.22E-43	5.94E-44	8.04E-43	1.10E-42
11	6.21E-44	8.93E-43	1.18E-42	8.65E-44	1.22E-42	1.69E-42
12	9.66E-44	1.45E-42	1.95E-42	1.21E-43	1.79E-42	2.52E-42
13	1.54E-43	2.42E-42	3.30E-42	1.68E-43	2.65E-42	3.80E-42
14	2.53E-43	4.18E-42	5.73E-42	2.40E-43	4.01E-42	5.85E-42
15	4.29E-43	7.35E-42	1.01E-41	3.60E-43	6.33E-42	9.34E-42
16	7.42E-43	1.30E-41	1.79E-41	5.75E-43	1.04E-41	1.54E-41
17	1.29E-42	2.27E-41	3.12E-41	9.65E-43	1.74E-41	2.58E-41
18	2.21E-42	3.90E-41	5.34E-41	1.66E-42	2.94E-41	4.34E-41
19	3.71E-42	6.56E-41	8.94E-41	2.84E-42	4.94E-41	7.24E-41
20	6.12E-42	1.08E-40	1.46E-40	4.82E-42	8.18E-41	1.19E-40
21	9.86E-42	1.72E-40	2.33E-40	8.01E-42	1.33E-40	1.92E-40
22	1.55E-41	2.70E-40	3.63E-40	1.30E-41	2.11E-40	3.03E-40
23	2.39E-41	4.13E-40	5.54E-40	2.06E-41	3.28E-40	4.69E-40
24	3.60E-41	6.19E-40	8.29E-40	3.18E-41	5.00E-40	7.11E-40
25	5.33E-41	9.10E-40	1.22E-39	4.82E-41	7.46E-40	1.06E-39
26	7.74E-41	1.32E-39	1.75E-39	7.15E-41	1.09E-39	1.55E-39
27	1.11E-40	1.87E-39	2.49E-39	1.04E-40	1.58E-39	2.22E-39
28	1.56E-40	2.63E-39	3.49E-39	1.49E-40	2.24E-39	3.14E-39
29	2.16E-40	3.63E-39	4.82E-39	2.10E-40	3.13E-39	4.38E-39
30	2.96E-40	4.96E-39	6.57E-39	2.91E-40	4.31E-39	6.03E-39

* Corresponding author.

E-mail address: jameel@giki.edu.pk

ORCID: 0000-0002-8229-8757 (Jameel-un Nabi), 0000-0003-4521-4259 (Muhammed Riaz), 0000-0002-2653-310X (Asim Ullah)

Table 3. Same as Table 2 but for ^{50}Fe and ^{54}Ni .

Energy (MeV)	^{50}Fe			^{54}Ni		
	T=0.5MeV	T=1.0MeV	T=1.5MeV	T=0.5MeV	T=1.0MeV	T=1.5MeV
2	8.34E-48	1.14E-46	1.49E-46	6.80E-48	1.20E-46	1.55E-46
3	1.97E-46	2.68E-45	3.49E-45	1.60E-46	2.81E-45	3.63E-45
4	1.35E-45	1.81E-44	2.36E-44	1.07E-45	1.88E-44	2.43E-44
5	5.33E-45	7.13E-44	9.28E-44	4.17E-45	7.28E-44	9.39E-44
6	1.54E-44	2.05E-43	2.67E-43	1.18E-44	2.06E-43	2.65E-43
7	3.63E-44	4.80E-43	6.25E-43	2.73E-44	4.73E-43	6.09E-43
8	7.39E-44	9.74E-43	1.27E-42	5.42E-44	9.40E-43	1.21E-42
9	1.35E-43	1.78E-42	2.31E-42	9.65E-44	1.68E-42	2.16E-42
10	2.27E-43	2.99E-42	3.90E-42	1.58E-43	2.78E-42	3.57E-42
11	3.57E-43	4.76E-42	6.22E-42	2.44E-43	4.36E-42	5.59E-42
12	5.35E-43	7.26E-42	9.53E-42	3.61E-43	6.60E-42	8.47E-42
13	7.74E-43	1.08E-41	1.43E-41	5.21E-43	9.88E-42	1.27E-41
14	1.10E-42	1.59E-41	2.11E-41	7.49E-43	1.49E-41	1.91E-41
15	1.54E-42	2.35E-41	3.14E-41	1.09E-42	2.27E-41	2.92E-41
16	2.16E-42	3.50E-41	4.71E-41	1.62E-42	3.54E-41	4.56E-41
17	3.07E-42	5.27E-41	7.14E-41	2.48E-42	5.60E-41	7.26E-41
18	4.44E-42	8.03E-41	1.09E-40	3.87E-42	8.97E-41	1.16E-40
19	6.52E-42	1.23E-40	1.69E-40	6.11E-42	1.44E-40	1.87E-40
20	9.70E-42	1.89E-40	2.60E-40	9.69E-42	2.29E-40	2.98E-40
21	1.46E-41	2.90E-40	3.98E-40	1.53E-41	3.61E-40	4.71E-40
22	2.19E-41	4.41E-40	6.05E-40	2.38E-41	5.60E-40	7.31E-40
23	3.27E-41	6.63E-40	9.09E-40	3.67E-41	8.56E-40	1.12E-39
24	4.86E-41	9.84E-40	1.35E-39	5.55E-41	1.29E-39	1.68E-39
25	7.15E-41	1.44E-39	1.98E-39	8.27E-41	1.90E-39	2.48E-39
26	1.04E-40	2.08E-39	2.85E-39	1.21E-40	2.76E-39	3.61E-39
27	1.49E-40	2.97E-39	4.06E-39	1.75E-40	3.96E-39	5.17E-39
28	2.12E-40	4.19E-39	5.72E-39	2.49E-40	5.59E-39	7.30E-39
29	2.97E-40	5.82E-39	7.94E-39	3.49E-40	7.78E-39	1.02E-38
30	4.11E-40	8.00E-39	1.09E-38	4.83E-40	1.07E-38	1.40E-38

4. Conclusion

GT transitions and ECC were calculated for selected fp-shell nuclei by using pn-QRPA model. Our calculated GT strengths results were bigger than previously measured and calculated results. The calculated ECC increases with the incident electron energy as well as with the core temperature. The increase in ECC due to temperature effect is in response of thermal unblocking of GT transitions states. These ECC study maybe of utility in the modeling and simulation of the pre-supernova evolution of massive stars.

Acknowledgments

J.-U. Nabi would like to acknowledge the support of the Higher Education Commission Pakistan through project numbers 5557/KPK /NRPU/R&D/HEC/2016, 9-5(Ph-1-MG-7)/PAK-

TURK /R&D/HEC/2017 and Pakistan Science Foundation through project number PSF-TUBITAK/KP-GIKI (02).

References

- [1] A. Staudt, E. Bender, K. Muto and H. V. Klapdor-Kleingrothaus, *At. Data. Nucl. Data. Tables*, (1990), 44, 79.
- [2] M. Hirsch, A. Staudt, K. Muto and H. V. Klapdor-Kleingrothaus, *At. Data and Nucl. Data Tables*, (1993), 53, 165-193.
- [3] J.-U. Nabi and H. V. Klapdor-Kleingrothaus, *Atom. Data and Nucl. Data Tables*, (2004), 88, 237.
- [4] J.-U. Nabi and H. V. Klapdor-Kleingrothaus, *At. Data Nucl. Data Tables*, (1999), 71, 149.
- [5] G. M. Fuller, W. A. Fowler and M. J. Newman, *Astrophys. J. Suppl. Ser.*, (1980), 42, 447; (1982), 48, 279; *Astrophys. J.* (1982), 252, 715; (1985), 293, 1.

- [6] K. Langanke and G. Martinez-Pinedo, Nucl. Phys. A (2000), 673, 481.
- [7] G. Martinez-Pinedo, K. Langanke and D. J. Dean, Astrophys. J. Suppl. Ser, (2000), 126, 493.
- [8] A. Heger, K. Langanke, G. Martinez-Pinedo and S. E. Woosley, Phys. Rev. Lett, (2001), 86, 1678.
- [9] D. J. Dean, K. Langanke, L. Chatterjee, P. B. Radha and M. R. Strayer, Phys. Rev. C, (1998), 58, 536.
- [10] D. Brink, D. Phil. Thesis, Oxford University, Unpublished (1955); P. Axel, Phys. Rev. (1962), 126, 671.
- [11] S. G. Nilsson, Mat. Fys. Medd. Dan. Vid. Selsk (1955), 29, 1.
- [12] K. Ikeda, S. Fujii and J. I. Fujita, Phys. Lett. (1963), 3 271.
- [13] I. Ragnarsson and R. K. Sheline, Phys. Scr. (1984), 29, 385.
- [14] P. Moller and J. Randrup, Nucl. Phys. A, (1990), 514, 1.
- [15] P. Moller, A. J. Sierk, T. Ichikawa and H. Sagawa, At. Data Nucl. Data Tables (2016), 109, 1.
- [16] G. Audi, F. Kondev, M. Wang, W. Huang, and S. Naimi, Chinese physics C, (2017), 41, 030001.
- [17] M. Hirsch, A. Staudt, K. Muto and H. V. Klapdor-Kleingrothaus, Nucl. Phys. A, (1991), 535, 62.
- [18] K. Muto, E. Bender and H. V. Klapdor, Z. Phys. A Atom. Nuc. A, (1989), 333, 125.
- [19] K. Nakamura, (Particle Data Group): J. Phys. G, Nucl. Part. Phys. (2010), 37, 075021.
- [20] N. B. Gove and M. J. Martin, At. Data Nucl. Data Tables (1971), 10, 205.
- [21] C. D. Goodman, C. A. Goulding, M. B. Greenfield, J. Rapaport, D. E. Bainum, C. C. Foster, W. G. Love and F. Petrovich, Phys. Rev. Lett, (1980), 44, 1755.
- [22] F. Molina, B. Rubio, Y. Fujita, W. Gelletly, J. Agramunt, A. Algora, J. Benlliure, P. Boutachkov, L. Cceres, R. B. Cakirli and E. Casarejos, Physical Rev. C, (2015), 91, 014301.
- [23] T. Adachi, Y. Fujita, P. Von Brentano, A. F. Lisetskiy, G. P. A. Berg, C. Fransen, D. De Frenne, H. Fujita, K. Fujita, K. Hatanaka and M. Honma, Physical Rev. C, (2006), 73 024311.
- [24] Y. Fujita, T. Adachi, P. Von Brentano, G. P. A. Berg, C. Fransen, D. De Frenne, H. Fujita, K. Fujita, K. Hatanaka, E. Jacobs and K. Nakanishi, Physical Rev. let, (2005), 95, 212501.
- [25] T. Adachi, Y. Fujita, P. Von Brentano, G. P. A. Berg, C. Fransen, D. De Frenne, H. Fujita, K. Fujita, K. Hatanaka, M. Honma and E. Jacobs, Nucl. Phys. A, (2007), 788, 70-75.
- [26] T. Adachi, Y. Fujita, A. D. Bacher, G. P. A. Berg, T. Black, D. De Frenne, C. C. Foster, H. Fujita, K. Fujita, K. Hatanaka and M. Honma, Phys. Rev. C, (2012), 85, 024308.
- [27] V. Kumar and P. C. Srivastava, The Eur. Phys. J. A 52 (2016) 181.